

TIME-RESOLVED MEASUREMENTS OF OVERLAYER ORDERING IN ELECTRODEPOSITION

A.C. Finnefrock*, L.J. Buller†, K.L. Ringland*, P.D. Ting‡, H.D. Abruña†, J.D. Brock‡

*Department of Physics, Cornell University, Ithaca, New York 14853

†Department of Chemistry, Cornell University

‡School of Applied and Engineering Physics, Cornell University

Abstract

We report *in situ* time-resolved surface x-ray scattering measurements of the underpotential deposition of Cu^{2+} on Pt(111) in the presence of Cl^- in HClO_4 solution. Chronoamperometric (current vs. time) measurements indicate that after a potential step, the electrodeposition current decays to $1/e$ of its initial value in at most 0.12 seconds. In contrast, our simultaneous time-resolved surface x-ray scattering data reveal that the overlayer requires on the order of two seconds to develop long-range periodic order. These results demonstrate that the kinetics of surface ordering can be significantly different from the kinetics of charge-transfer and illustrate the power of time-resolved surface x-ray scattering for *in situ* studies of electrodeposition.

Introduction

The electrodeposition of a metal adsorbate onto a solid surface is a key aspect of important technological processes such as electroplating and corrosion inhibition. In a number of cases, metal overlayers can be electrodeposited onto a dissimilar metal substrate at a potential that is less negative than the Nernst potential (that required for bulk deposition). Experimentally, this “underpotential deposition” (UPD) provides a precise means for quantitatively and reproducibly controlling coverage in the submonolayer to monolayer (and in some cases multilayer) regime [1–3]. In addition to the surface coverage, both the presence of other adsorbates, especially anions, and the surface structure of the substrate can profoundly affect the structural and electronic characteristics of the deposit [4–8]. Although there is a great deal of existing work on UPD lattice formation, the early stages of deposition are not well-understood [9, 10]. In much of this earlier work, the structure of a UPD overlayer was determined by depositing the overlayer followed by emerging into an ultra-high vacuum (UHV) chamber and employing established surface science techniques such as low-energy electron diffraction (LEED). However, such measurements are inherently *ex situ* and cannot provide information on the kinetics of deposition. Recently, *in situ* probes such as scanning tunneling microscopy (STM) [11–13], atomic force microscopy (AFM) [14], and surface x-ray scattering (SXS) [15–20] have been applied to UPD systems. In addition to eliminating the ambiguity of *ex situ* measurements, they offer the possibility of studying the kinetics of deposition. Kinetic studies are crucial for identifying the rate-limiting steps in the electrochemical growth.

The UPD of Cu onto Pt(111) has been extensively studied by a variety of techniques. The process is very sensitive to the presence of anions and appears to be kinetically controlled. The exact structure and nature of the overlayer, particularly at intermediate coverages, has been the subject of some controversy. Based on LEED studies, Michaelis *et al.* [21] identified

the intermediate overlayer as a 4×4 structure. However, *in situ* anomalous x-ray diffraction measurements of the overlayer structure as a function of potential by Tidswell *et al.* [22] suggest that the intermediate overlayer structure is a more complicated incommensurate CuCl bilayer.

Time-resolved surface x-ray scattering is a nearly ideal probe for studying the time evolution of the overlayer structure during UPD. This is a noninvasive technique which can simultaneously measure from a broad area on the sample, in marked contrast to scanning probe techniques. X rays in the 0.5 to 1.5 Å region are not significantly absorbed by aqueous solutions allowing for the *in situ* study of the electrode/solution interface. In addition, the line shape of the scattered x rays can be interpreted simply in terms of well-known correlation functions, allowing direct tests of theory. Using signal averaging techniques, transient structures with lifetimes as short as a few μsec can be studied [23].

Experiment

Experiments were performed at the X20A beamline at the National Synchrotron Light Source using an *in situ* reflection-geometry x-ray scattering cell. This cell is an adaptation of the design originally developed by Toney [24]. All values of the applied voltage are referenced to a Ag/AgCl reference electrode. Our sample was a single-crystal Pt(111) electrode, immersed in a solution of 1 mM Cu^{2+} and 10 mM Cl^- with 0.1 M HClO_4 as a supporting electrolyte. Polypropylene film was used to cover the sample and contain the solution, as depicted in Figure 1(a). During the experiment, chronamperometric measurements were synchronized with the time base of a multi-channel scalar, which recorded the intensity of the scattered x rays. We were thereby able to acquire simultaneous *in situ* time-resolved measurements of x-ray scattered intensity and charge-transfer.

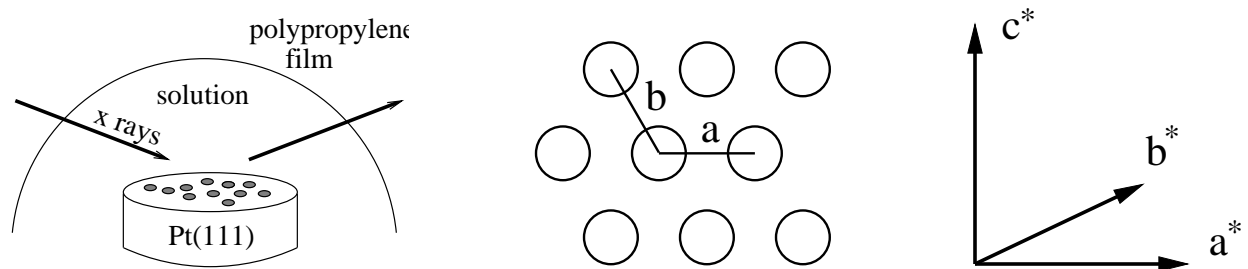


Figure 1: (a) Cartoon of the *in situ* x-ray scattering cell. X rays penetrate the polypropylene film and solution to diffract from the ordered monolayer structure on the electrode surface. (b) The Pt(111) surface with surface lattice vectors **a**, **b**, which are perpendicular to **c** = (111). (c) Reciprocal lattice vectors corresponding to the unit cell chosen in (b); **a*** and **b*** subtend 60° .

Since we will be discussing structural measurements referenced to the platinum surface, a brief description of the crystallographic notation is in order. Platinum has a face-centered cubic (fcc) crystal structure with a cubic lattice spacing of 3.9231 Å. The bulk-terminated (111) surface of platinum has sixfold symmetry; therefore, in most surface diffraction studies, the crystal lattice is described in terms of a hexagonal lattice with the **c** axis along the $\langle 111 \rangle$ direction. Thus the fcc (111), (200), and (020) Bragg peaks are respectively mapped onto the (003), (1 $\bar{1}$ 2), and (012) in surface units. A more thorough description can be

found in Reference [25]. Points in reciprocal space are usually indexed by (HKL) , where the momentum transfer vector is $q = H\mathbf{a} + K\mathbf{b} + L\mathbf{c}$.

Figure 2 represents the present understanding [21,22] of the UPD of Cu/Cl onto Pt(111). There are three distinct equilibrium phases, here labeled A, B, and C. At the rest potential, Cl^- is adsorbed onto the electrode in an amorphous state. As the applied potential is ramped negatively, a current peak is observed. Beyond this peak, the Cu and Cl form an incommensurate “overlayer” pattern which is well-ordered. This is phase (B). As the applied potential is again ramped negatively, the current again peaks, signalling the transition to another phase (C). Here, the Cu and Cl form a tighter overlayer structure which is commensurate with the Pt(111) electrode substrate. If the potential is ramped positively towards the rest potential, current peaks are found which correspond to transitions between the phases, now in the opposite direction.

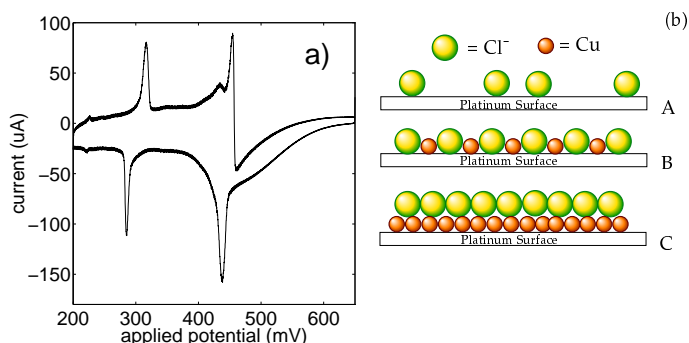


Figure 2: (a) An *in situ* (in the x-ray cell) cyclic voltammogram at 5 mV/second for Cu UPD on Pt(111) in 0.1 M HClO_4 solution containing 1 mM Cu^{2+} and 10 mM Cl^- . (b) Schematic depiction of the electrodeposition process moving from a disordered chloride layer (A) to a Cu and Cl^- overlayer with long-range order (B) and finally to a full Cu monolayer (C) as the potential is made progressively more negative.

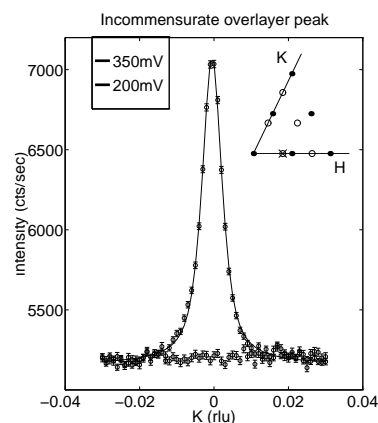


Figure 3: Comparison of the scattered x-ray intensity at the $(0.765\ 0\ 1.5)$ incommensurate overlayer diffraction peak (shown by a cross in the inset) in the two distinct phases, corresponding to the incommensurate overlayer (350 mV) where the peak is present, and commensurate overlayer (200 mV) where the peak is absent. The solid line is a fit to a pseudo-Voigt lineshape, to guide the eye.

Results

This paper concentrates on the transition between phases (B) and (C). That is, we are studying the transition between two ordered phases as a function of applied potential. In the former phase (B), the CuCl overlayer has a lattice spacing approximately 30% greater than the lattice spacing between Pt atoms on the (111) surface [22]. Hence, rods of scattering which are sharp in the \mathbf{a}^* and \mathbf{b}^* direction but diffuse in the \mathbf{c}^* direction should be observable. The intensity along \mathbf{c}^* is not entirely uniform; its modulation can provide information about the spacing between the Cu and Cl planes in the overlayer. In the latter phase (C), the CuCl overlayer is commensurate with the Pt(111) rod. So the rod of scattering from the overlayer

interferes with the scattering from the crystal truncation rods (CTR) of the Pt(111) surface [26]. This makes the interpretation of changes in intensity more complicated. Nonetheless, these modulations of the CTRs are easily observable and can be fit to provide structural information on this phase as well. This analysis is greatly simplified by the fact that Pt(111) is known not to reconstruct in this potential window.

Figure 3 shows the scattering found at the $(0.765\ 0\ 1.5)$ position at two different values of the applied potential, clearly demonstrating the presence of the incommensurate overlayer structure at a higher value of the applied potential and its absence at a lower value corresponding to the commensurate structure. The full width at half maximum of this peak corresponds to a coherence length of at least 120\AA . The potential-independent background shown in this figure is due to scattering from the solution and the polypropylene film.

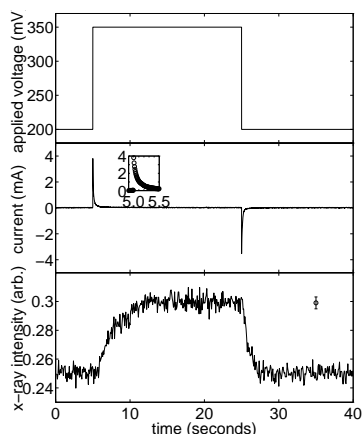


Figure 4: (a) Applied potential steps. (b) Transient currents observed when this potential step sequence is performed. (c) Simultaneous *in situ* X-ray scattered intensity of the overlayer diffraction peak as a function of time. The development of long-range periodic order in the overlayer (panel c) requires significantly more time than that required for the charge-transfer at the electrode surface (panel b).

To study the kinetics of the Cu/Cl/Pt(111) UPD process, we performed the applied potential square-wave cycle shown in Figure 4(a). Initially, the potential began at 200 mV where there is a CuCl overlayer commensurate with the Pt(111) electrode surface (phase C). Then at $t = 5$ seconds, the potential was stepped to 350 mV, conducive to the formation of an incommensurate CuCl overlayer (phase B). At $t = 25$ seconds, the potential was stepped back to the original 200 mV. This cycle was repeated ten times to gather statistics for the simultaneous x-ray measurement.

Figure 4(b) shows the transient currents observed when this potential step sequence is performed. These currents are generated by the stripping of Cu^{2+} and/or the adsorption of Cl^- on the positive potential step and the reverse for the negative potential step. The area under each current transient represents the total charge transferred during the process and can be used to identify the electrochemical process. For each step, the total charge transfer

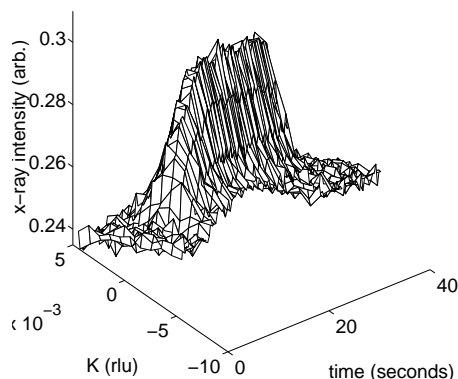


Figure 5: Scattered intensity as a function of time t and scattering vector, $\mathbf{q} = (0.765\ K\ 1.5)$. The peak remains centered at $k = 0$, ruling out the possibility that the overlayer simply shifts its periodicity in response to the voltage stimulus.

is $\lesssim 1$ mC. The time for the current to fall to $1/e$ of its original value is 0.08 seconds for the positive step, and 0.12 seconds for the negative step. These time scales are too slow, and the charge transfers too large, to be explained by charging of the double-layer. However, these parameters are completely consistent with the UPD processes depicted in Figure 2(b).

Time-resolved x-ray data were acquired simultaneously with these chronoamperometric measurements. These data are presented in Figure 4(c) which shows the intensity of the (0.765 0 1.5) overlayer diffraction peak as a function of time. A representative error bar is displayed in the upper right-hand corner. Hence, the fluctuations in the measured intensity can be seen to arise from counting statistics. These intensities were fit to an exponential line shape for the purpose of estimating time constants. The intensity rise at $t = 5$ seconds, due to the formation of an ordered overlayer, has a time constant of 2.3 seconds. In contrast, the intensity fall at $t = 25$ seconds has a characteristic time constant of 0.75 seconds. This demonstrates that the ordering process for the incommensurate overlayer is slower than its disordering, an intuitively pleasing result. What is more surprising is the enormous discrepancy in time scales between the charge-transfer shown in panel (b) and the x-ray scattering signal in panel (c). Clearly, the development of long-range periodic order in the overlayer requires significantly more time than that required for the charge-transfer. Thus, charge-transfer at the electrode surface is not the rate-limiting process.

One contingency that must be allowed for is the possibility that the peak could be moving in H or K . At the (0.765 0 L) position, this would correspond to the overlayer expanding/contracting or rotating with respect to the underlying platinum lattice. Hence, it is necessary to take time-resolved q -scans, rather than simply monitoring the intensity at a single point in reciprocal space. A representative q - t -scan is shown in Figure 5. From these and similar scans, the peak is simply appearing and disappearing, and not altering its periodicity in a continuous manner. This indicates the slow and uniform ordering of the incommensurate overlayer and its more rapid dissolution, in agreement with the results for the peak intensity shown in Figure 4.

Conclusions

In summary, by combining chronoamperometric measurements with time-resolved surface x-ray scattering, we have demonstrated that the transfer of charge during the deposition and stripping process is far more rapid than the time required to form an ordered CuCl overlayer. Electrochemical measurements alone are insufficient to determine the rate-limiting steps in this UPD system. This illustrates demonstrate the power of time-resolved x-ray scattering as an *in situ* probe of the kinetics of UPD processes in particular, and of interfacial growth in general.

Given the success of these experiments, we are currently carrying out further measurements to probe the height-height correlation function throughout the underpotential deposition cycle. Detailed line shape analysis will provide information on the time-dependent order parameter and correlation lengths along the surface. For instance, monitoring peak widths (such as shown in Figure 5) yields domain sizes of growing islands on the surface as a function of time. These studies will further elucidate the microscopic details of surface and interface evolution.

Acknowledgements

This work was supported by Cornell's Materials Science Center (MRL program of the NSF under Grant No. DMR-9121654). Additional support was provided by the NSF (Grant Nos. DMR-92-57466 and CHE-94-07008) and the Office of Naval Research. The x-ray data were collected using the IBM-MIT beam line X20A at the National Synchrotron Light Source (NSLS), Brookhaven National Laboratory. LJB acknowledges support of a fellowship from the International Precious Metals Institute / Gemini Industries. ACF would like to thank the organizers of this symposium for support to attend the MRS conference, and M. Toney and B. Ocko for helpful discussions.

References

- [1] D. Kolb, in *Advances in Electrochemistry and Electrochemical Engineering*, edited by H. Gerisher and C. Tobias (Wiley and Sons, New York, 1978), Vol. 11.
- [2] R. Adžić, *Isr. J. Chem.* **18**, 166 (1979).
- [3] S. Szabó, *Int. Rev. Phys. Chem.* **10**, 207 (1991).
- [4] D. Kolb, A. Jaaf-Golze, and M. S. Zei, in *Dechema Monographien* (VCH, Germany, 1986), Vol. 102, pp. 53–64.
- [5] J. H. White and H. D. Abruña, *J. Phys. Chem.* **94**, 894 (1990).
- [6] N. Marković and P. N. Ross, *Langmuir* **9**, 580 (1993).
- [7] J. H. White and H. D. Abruña, *J. Electroanal. Chem.* **300**, 521 (1991).
- [8] R. Gómez, J. Feliu, and H. Abruña, *Langmuir* **10**, 4315 (1994).
- [9] J. Schultze and D. Dickertmann, *Surf. Sci.* **54**, 489 (1976).
- [10] A. Bewick and B. Thomas, *J. Electroanal. Chem.* **70**, 239 (1976).
- [11] O. Magnussen *et al.*, *Phys. Rev. Lett.* **64**, 2929 (1990).
- [12] G. Edens, X. Gao, and M. Weaver, *J. Electroanal. Chem.* **375**, 357 (1994).
- [13] T. Hachiya, H. Honbo, and K. Itaya, *J. Electroanal. Chem.* **315**, 275 (1991).
- [14] S. Manne *et al.*, *Science* **251**, 183 (1991).
- [15] O. Melroy *et al.*, *Phys. Rev. B* **38**, 10962 (1988).
- [16] M. Toney *et al.*, *Phys. Rev. B* **42**, 5594 (1990).
- [17] M. Toney *et al.*, *Phys. Rev. Lett.* **75**, 4472 (1995).
- [18] J. Wang, A. Davenport, H. Isaacs, and B. Ocko, *Science* **255**, 1416 (1992).
- [19] J. Wang, B. Ocko, A. Davenport, and H. Isaacs, *Phys. Rev. B* **46**, 10321 (1992).
- [20] B. Ocko, G. Watson, and J. Wang, *J. Phys. Chem.* **98**, 897 (1994).
- [21] R. Michaelis, M. Zei, R. Zhai, and D. Kolb, *J. Electroanal. Chem.* **339**, 299 (1992).
- [22] I. Tidswell, C. Lucas, N. Marković, and P. Ross, *Phys. Rev. B* **51**, 10205 (1995).
- [23] E. Sweetland *et al.*, *Phys. Rev. B* **50**, 8157 (1994).
- [24] M. Samant *et al.*, *Surf. Sci. Lett.* **193**, L29 (1988).
- [25] A. Sandy *et al.*, *Phys. Rev. B* **43**, 4667 (1991).
- [26] I. Robinson, in *Handbook on Synchrotron Radiation*, edited by G. Brown and D. Moncton (Elsevier Science Publishers B.V., Amsterdam, 1991), Vol. 3, Chap. 7.